Projection-based order reduction of a nonlinear biophysical neuronal network model

Mikko Lehtimäki, Lassi Paunonen and Marja-Leena Linne

Abstract— In this study mathematical model order reduction is applied to a nonlinear model of a network of biophysically realistic heterogeneous neurons. The neuron model describes a pyramidal cell in the hippocampal CA3 area of the brain and includes a state-triggered jump condition. The network displays synchronized firing of action potentials (spikes), a fundamental phenomenon of sensory information processing in the brain. Simulation of the system is computationally expensive, which limits network size and hence biological realism. We reduce the network using advanced variations of Proper Orthogonal Decomposition and Discrete Empirical Interpolation Method. The reduced models should recreate the original spiking activity. We show that reduction methods with online adaptivity achieve the most accurate reduction results. Some of the reduced models consume less computational resources than the original, at the cost of changes in population activity of the tested network model.

I. INTRODUCTION

In the field of neuroscience, there is a great demand to incorporate molecular and cellular level detail in large-scale models of the brain in order to recreate phenomena such as learning and behavior [9]. This cannot be achieved with the computing power available today, since detailed models are complex and often computationally too demanding for large-scale network or system level simulations. Model order reduction (MOR) is a mathematical method for improving computational efficiency of simulations of mathematical models. However, in computational neuroscience the use of MOR is not common. Instead, efficient models are typically derived by eliminating variables and making assumptions of system behavior.

Neuronal activity can be modeled in detail with the Hodgkin-Huxley (HH) formalism [10]. Less detailed, simplified neuron models are motivated by computationally efficient large scale simulations [11]. Morphologically accurate models of branching neurons have been simplified algorithmically to derive efficient models [15], [16]. However, the simplification approach is not suitable for the current trend in neuroscience, in which multiple physical scales of the brain are incorporated in simulations and the consequent analysis of neural phenomena. Instead comprehensive models with full system dynamics are needed in order to increase understanding of different actors in one brain area.

In this paper, we study the effectiveness of MOR methods to reduce a nonlinear biophysical network model describing synchronized population bursting behavior of heterogeneous pyramidal neurons in the brain [21]. Modeling studies in computational neuroscience are typically interested in the spatial and temporal evolution of the membrane voltage of neurons. Neurons communicate by swiftly changing their membrane voltage to create action potentials (spikes) that propagate from cell to cell. Spiking is the fundamental method of sensory information processing in the brain, and synchronized spiking is an emergent property of biological neuronal networks. MOR should preserve this network behavior. Here we reduce the network model with four variations of Proper Orthogonal Decomposition (POD) [14] and Discrete Empirical Interpolation Method (DEIM) [4] that are developed to reduce nonlinear systems. These methods are DEIM, Localized DEIM (LDEIM) [18], Discrete Adaptive POD (DAPOD) [28] and Adaptive DEIM [20]. DEIM and the variations are used here in combination with POD.

The neurons in our network model feature a state-triggered jump condition. Such *resets* are often used in simplified neuron models to efficiently simulate the spiking behavior of a neuron [11] as an alternative to explicitly modeling ion channel kinetics. In the present model, the jump condition implements a biological boundary to ions that are in limited supply in the neural matter.

Many versions of DEIM have been developed. Unassembled DEIM improves the reducibility of finite element models [24]. Matrix DEIM improves the efficiency of evaluating the Jacobian matrix [26]. Localized DEIM uses machine learning to compute multiple reduced bases offline and choose between them in the online phase appropriately [18]. Temporally Localized DEIM, a recent approach to rapidly changing local subspaces was introduced in [3]. Adaptive DEIM with online updates to the DEIM basis and interpolation points has been developed to better handle unseen states in the simulation phase [20]. Non-negative DEIM adds structure preservation guarantees to the reduced model [1]. Furthermore, several recent studies address the performance of DEIM in noisy environments and propose randomized oversampling and QR-decomposition inspired basis computation methods [6], [19]. Finally, an algorithm that adapts the POD basis online, Discrete Adaptive POD, has been published [29]. It can be combined with many of the DEIM algorithms. Our reduction methods in choice are described in detail in Section III.

M. Lehtimäki: Computational Neuroscience, Faculty of Medicine and Health Technology, Tampere University. Supported by TUNI Graduate School. `mikko.lehtimaki@tunif.i`

L. Paunonen: Mathematics, Faculty of Information Technology and Communication Sciences, Tampere University. Supported by Academy of Finland grants 298182 and 310489. `lassi.paunonen@tuni.fi`

M-L. Linne: Computational Neuroscience, Faculty of Medicine and Health Technology, Tampere University. Supported by Academy of Finland grant 297893 and Human Brain Project (785907). `marja-leena.linne@tunif.i`

Mathematical MOR of nonlinear systems in neuroscience has been studied before in limited settings. Kellems et al. (2010) reduced a partial differential equation (PDE) model that described a single branching neuron with HH dynamics [12]. They compared how an action potential travels from stimulus injection point along the neuron in the original and reduced models, using POD-DEIM as the MOR method. Du et al. (2014) built on the work of Kellems et al. by including linearization of weakly excitable (passive) parts of the neuron [7]. Amsallem and Nordström (2016) studied a branching neuron and introduced stability and nonnegativity properties to the reduced basis [1]. Finally, Lehtimäki et al. (2017) reduced a chemical reaction based nonlinear model of synaptic plasticity [13] using POD-DEIM.

Nonlinear MOR studies of population activity of neurons have been conducted to model the cardiac and muscular systems. A model of electrical properties of the cardiac system has been reduced in [2] via POD and in [27] via POD-DEIM. Both studies used a simple phenomenological neuron model. Additionally, POD-DEIM has been employed in reduction of bidomain and monodomain electromyography models describing muscle fibers in [17], [8], where the more biophysically accurate HH formalism was employed.

In Section II we describe the biophysics and construction of the network model. Section III explains our MOR approach and methods in more detail. Our results are presented in IV and we conclude by discussing the significance of our work and ideas for future studies in sections V and VI, respectively.

II. BIOPHYSICAL NETWORK MODEL

The biophysical network model describes pyramidal neurons from the CA3 area of the hippocampus [21]. The morphology of the cell is considered by a spatial modeling approach, where the cell is split into compartments, and the membrane voltage of each compartment is coupled with the voltage of adjacent compartments via electrotonic coupling as described by the neuronal cable theory [22]. Each neuron is modeled in a biophysical manner, so that the membrane voltage of one compartment behaves according to ionic currents in HH formalism [10]. Ion channels model the *active* propagation, and cable theory models the *passive* propagation of membrane potential along the cell. The single-cell model itself is a simplified version of an originally 19 compartment model of the same cell type [25].

A network of these cells is formed by coupling them in a random, directed graph manner. The interesting property of the modeled network is its capability to bring about and sustain periodic, oscillating population level activity, where neurons spike in their somas in a synchronized manner. We wish to determine whether this behavior is preserved throughout the MOR process.

Each single cell model consists of ten ordinary differential equations (ODEs). The ODE of the somatic membrane potential V_s is

$$C_m \frac{dV_s}{dt} = - I_{leak}(V_s) - I_{Na}(V_s, m, h) - I_{K-DR}(V_s, n) + \frac{g_c}{p}(V_d - V_s) + \frac{I_s}{p},$$

(1)

where V_d is the voltage of the dendritic compartment, I_{leak} is a leak current, I_s is an injected current, I_{Na} is a sodium current, I_{K-DR} is a potassium delayed rectifier current, m, h and n are HH-type voltage gated ion channel activation variables of sodium and potassium (delayed rectifier), g_c is the electrotonic coupling conductance between the two compartments and p is the relative size of the soma compartment.

The ODE of the dendritic compartment is comparable to the somatic compartment, however in place of sodium currents and potassium delayed rectifier current the voltage of the dendritic compartment depends on calcium, calcium-activated potassium and afterhyperpolarization potassium currents. Their respective activation variables are s, c and q. Additionally, excitatory synaptic currents from NMDA (S) and AMPA (W) are included. Moreover, Ca in the dendritic compartment as well as the synaptic AMPA and NMDA concentrations are modeled with their respective ODEs. [21]

The kinetics of the gating variables h, n, s, c and q are modeled by ODEs of the form

$$\frac{dy}{dt} = (y_\infty(U(t)) - y)/\tau_y(U(t)),$$

(2)

where $U(t)$ is either the somatic or dendritic membrane voltage or calcium (Ca) concentration at time t, depending on the gating variable, and

$$y_\infty = \alpha_y/(\alpha_y + \beta_y)$$

(3)

and

$$\tau_y = 1/(\alpha_y + \beta_y)$$

(4)

where α_y and β_y are distinct for every gating variable m, h, n, s, c. For example, for gating variable n we have

$$\alpha_n = \frac{0.016(35.1 - V_s)}{e^{(35.1-V_s)/5-1}},$$
$$\beta_n = 0.25 e^{0.5 - 0.025 V_s},$$

hence the model contains very fast nonlinear dynamics. The sodium activation gate m is instantaneous and is modeled only with Equation 3.

The ODE of the NMDA concentration is particularly interesting as it is connected to a reset condition that keeps the value of S bounded so that

$$\frac{dS}{dt} = \sum jH(V_{s,j} - 10) - S/150,$$
$$S(t) = \min(S(t), 125),$$

(5)

where $V_{s,j}$ is the somatic voltage of the synaptic connection from cell j and $H(x) = 1$ if $x \geq 0$ and 0 otherwise. The constants keep $S(t)$ in a biologically justified range. From this equation the nonlinear nature of synaptic connections is also apparent. For full details of the single cell model,

see [21] and for an implementation that accounts for the errata of the original publication, see [5].

Our network model consists of heterogeneous neurons. The calcium conductance in the dendritic compartment can vary by 10%, with the amount drawn from the uniform distribution. Each cell receives synaptic input from 20 other randomly chosen cells. We use in total 50 cells, obtaining an ODE system of 500 variables. To study the population behavior we use numerical integration with fixed step 4th order Runge-Kutta method. One cell is stimulated with a current pulse at $t = 5\,\text{ms}$ for $t = 50\,\text{ms}$ and the simulation is executed for $1000\,\text{ms}$ with a timestep of $dt = 0.02\,\text{ms}$. To measure population behavior, at each time instance the number of cells that are spiking is counted. An action potential (membrane voltage spike) is considered to occur when a threshold level is exceeded. Here, the threshold is $V_t = -40\,\text{mV}$, as in [21].

The network model we study is nonlinear with

$$x'(t) = Ax(t) + f(x(t)) + Bu(t), \qquad (6)$$

where A is the state matrix, B is the input matrix, $u(t)$ is a vector of time dependent inputs and $f(x(t))$ is a vector of nonlinear functions. $A \in \mathbb{R}^{10\nu \times 10\nu}$ and $B \in \mathbb{R}^{10\nu \times 4\nu}$ are block diagonal matrices composed of the state and input matrices of the cells in the network, and $f(x(t)) \in \mathbb{R}^{10\nu}$, where ν is the number of cells in the network. The system has a stable steady state where each cell in the network is at resting potential, thus no cell is spiking, and if the system is stimulated with current injection every cell will eventually return to the resting potential after the stimulus has stopped.

III. MODEL ORDER REDUCTION

We create reduced order models (ROMs) with variations of POD [14] and DEIM [4]. These methods are applicable to general nonlinear systems and their suitability to models with Hodgkin-Huxley type ion channel kinetics has been studied before in [1], [7], [8], [12], [17]. Furthermore, we wish to avoid linearizations, since for the present system it is very challenging to determine robust linearization points. These methods also allow the implementation of reset conditions that are a part of the studied model, similarly as in [2].

POD is a projection based MOR method that approximates the original n dimensional system in a reduced order linear subspace. A reduced basis with orthonormal column vectors $V_k \in \mathbb{R}^{n \times k}$ where $k < n$ is determined using singular value decomposition (SVD). This POD basis is constructed from snapshots $Y = [y_1, y_2, \cdots, y_s]$ that are a set of solutions to the original system [23]. By setting $x(t) \approx V_k \tilde{x}(t)$ and projecting the system described in Equation 6 onto V_k by Galerkin projection, a reduced system

$$\tilde{x}'(t) = \underbrace{V_k^T A V_k}_{\tilde{A}} \tilde{x}(t) + V_k^T f(V_k \tilde{x}(t)) + \underbrace{V_k^T B}_{\tilde{B}} u(t) \qquad (7)$$

is obtained. In Equation 7 $\tilde{A}$ and $\tilde{B}$ can be precomputed before the online (simulation) phase. However, while POD itself can be applied to nonlinear systems, there is no guarantee of computational savings as the nonlinear part of the system must be evaluated in the original space.

Efficient evaluation of the nonlinear term can be achieved with DEIM [4]. DEIM extends the subspace projection approach of POD with an interpolation step for nonlinear functions. To construct a reduced order approximation of the nonlinear vector, the algorithm determines

$$\tilde{f}(x,t) \approx U_m (P_m^T U_m)^{-1} P_m^T f(x,t), \qquad (8)$$

where the DEIM basis $U_m = [u_1, u_2, \cdots, u_m], m < n$ is determined via SVD of snapshots of nonlinear function outputs, $P_m^T f(x,t) := f_m(x,t)$ is a nonlinear function with m components chosen from f according to DEIM determined interpolation points $p_1, \cdots, p_m$ and $P_m = [e_{p_1}, e_{p_2}, \cdots, e_{p_m}]$ with e_{p_i} being the standard basis vector i of $\mathbb{R}^n$. Note that the POD dimension k and DEIM dimension m do not need to be equal, although empirically it has been observed that $k = m$ leads to most accurate reduced models [8], [19]. Together POD and DEIM form a ROM

$$\tilde{x}'(t) = \tilde{A}\tilde{x}(t) + \underbrace{V_k^T U_m (P^T U_m)^{-1}}_{N} f_m(V_k \tilde{x}(t)) + \tilde{B}u(t),$$
$$(9)$$

where N can be precomputed in the offline phase. Thus in the online phase it remains to compute $V_k \tilde{x}$ so that f_m can be evaluated at the m interpolation points.

Each cell in the network model has a state determined jump condition, as seen in Equation 5. This condition must be checked at every evaluation of the state of the system. To determine the jump condition, the reduced state vector $\tilde{x}$ must be projected to the original space. Numerically we implement this check before every evaluation of the nonlinear vector $f_m(x,t)$, that also requires the state in the original space. However, after resolving jump conditions the state needs to be projected back to the reduced space in order to evaluate $\tilde{A}\tilde{x}$, which creates an extra computational step that would not be otherwise required. The cost of this step depends on the chosen POD dimension k.

A. Versions of the Discrete Empirical Interpolation Method

In addition to DEIM as described in [4] we test the efficacy of Localized Discrete Emprical Interpolation Method (LDEIM) [18]. In LDEIM, a clustering algorithm is employed in the offline phase to group solution snapshots before DEIM basis generation. Several bases and interpolation points $(U_{m_1}, P_{m_1}), \cdots, (U_{m_p}, P_{m_p})$ are computed to obtain a set of local bases, one from each cluster of snapshots, in contrast to the global basis used in DEIM. Each local basis has the same dimension, and LDEIM should achieve a similar error estimate as a global basis but with a smaller dimension. In the online phase a local precomputed DEIM basis is chosen adaptively. The features used to derive and choose the bases are a subset of outputs from the nonlinear function. LDEIM requires the number of clusters and features as user defined parameters, and the size of the feature vector is a decision between classification power and computational efficiency. The premise of LDEIM is

to use multiple smaller yet accurate reduced subspaces to compensate for the extra online computation time that is needed for basis selection.

Another further development of DEIM that we use is Adaptive DEIM (ADEIM) [20]. In ADEIM, the DEIM basis and interpolation points are updated online. Initially, (U_m, P_m) are computed offline, and at step s of the simulation (U_s, P_s) are determined. The adaptivity is performed via low-rank updates to (U_{s-1}, P_{s-1}). A random set of size s_p of unique additional sampling points of the nonlinear function is drawn from the uniform distribution and added to the set of total sampling points, then the nonlinear function is evaluated at these points in length w window of past solutions. The resulting online snapshots are used to compute an updated basis and sampling points. This online adaptivity does not change the dimension of the reduced subspace. The algorithm involves considerable online computation, but is more capable of reducing models with trajectories that were not sampled in the offline phase.

Finally, we implement Discrete Adaptive POD (DA-POD) [29], [28] with DEIM. DAPOD adapts the dimension and structure of the POD basis V online. In the online phase, new snapshots are incorporated and existing ones eliminated from the snapshot ensemble based on adaptivity criteria that weigh importance and age of snapshots. The basis size is determined with an error bound parameter ϵ decided by the user. A smaller ϵ corresponds to a tighter error bound, which results in a larger POD dimension and greater run time. DAPOD can be combined with DEIM to reduce nonlinear models more efficiently. However, as the POD basis V now changes online, the DEIM projection matrix N of Equation 9 cannot be precomputed, which adds some additional online computational burden.

IV. RESULTS

The network displays a temporally synchronized activity pattern, where the majority of the neurons spike at similar times, which replicates the behavior from [21]. This is seen as oscillations in the number of neurons spiking at any given time. Figure 1 illustrates the trajectory of the somatic membrane voltage of the stimulated neuron (top) along with network level activity (bottom) as a raster plot. In the raster plot, a red dot is marked at every time instance on the x-axis if the somatic voltage of a neuron in the y-axis is greater than a voltage threshold $V_t = -40$ ms. The stimulated neuron is at index 0 in the raster plot.

The oscillations of the population activity are an important phenomenon of the model and one that the ROM should recreate. The pattern is illustrated in Figure 2, which shows the number of neurons spiking as a function of time. A qualitative comparison of the original model to reduced order models of several parameters, with many reduction methods, is provided in Figure 2. The behavior of the original model is shown in every plot, and each row corresponds to a different reduction method. Combinations of dimensions or reduction method specific parameters are displayed in different colors.
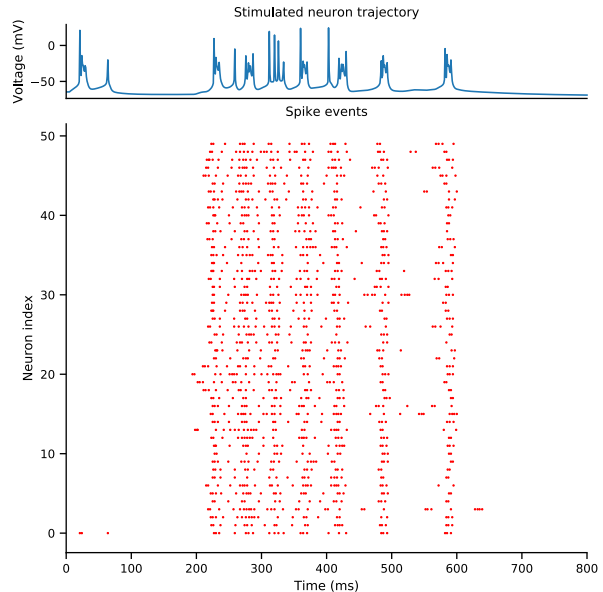

Fig. 1. Top: trajectory of the somaticmembrane voltage of the stimulated neuron. Bottom: raster plot of spike events of each neuron as a function of time.

In Figure 2 it is seen that each reduction method has their strengths and weaknesses in recreating the original simulation. With the present model, a 5-10% reduction, depending on the method, causes numerical overflow errors or flat trajectories. The overflow errors end the simulation immediately, and a ROM with a flat trajectory is not useful. For this reason, the analysis considers DEIM dimensions 480 and 470.

The top most plot in Figure 2 presents the performance of the standard DEIM method from [4]. Notably, the reduced order models display a slight temporal shift in population activity around $t = 600$ ms already with 4% reduction. Moreover, an additional burst of spikes at $t = 750$ ms is detected and subsequent residual network activity is observed in the DEIM reduced models, although the original network silences itself after the last population burst. This method has the lowest computational burden and even with the current slight reduction is faster to simulate than the original model.

The second plot from the top in Figure 2 shows results obtained with the LDEIM method from [18]. The trajectories are very similar to original DEIM, although LDEIM produces the early network activity more accurately. Both methods show a shift in the times of occurrence and magnitudes of synchronized spike events as the simulation progresses. Residual network activity is also observed here. The simulation time of LDEIM is greater than DEIM, since with the present model LDEIM does not achieve a smaller dimension than DEIM and the overhead of online basis changes reduces the computational efficiency of the reduced models.

Results with the DAPOD-DEIM method from [29], [28] are shown in the third plot from the top in Figure 2. DAPOD
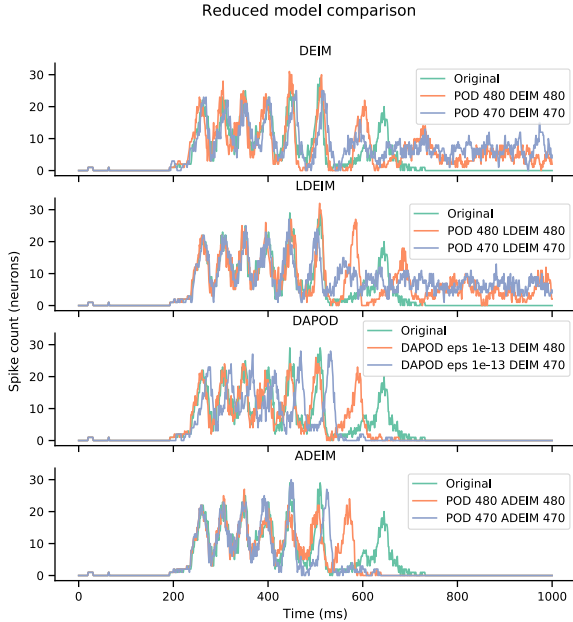
Fig. 2. Comparison of population behavior with different reduction methods and parameters. Methods from top to bottom are DEIM, LDEIM, DAPOD-DEIM and ADEIM. In all plots, x-axis is time in milliseconds and y-axis is number of neurons spiking.

is unique in the set of tested methods because it allows the POD basis to change online phase of reduction. We keep the error controlling value ϵ constant while lowering the DEIM dimension. In our simulations, this online adaptivity allows DAPOD to use a smaller number of POD dimensions than what is achieved by other reduction methods. With $\epsilon = 1e^{-13}$ the POD dimension is in the range $[462, 456]$. It is seen that at 470 DEIM dimensions, DAPOD-DEIM fails to recreate the last spike in population activity, whereas DEIM set to 480 displays it, although with a temporal and magnitudinal shift. Remarkably, DAPOD-DEIM simulations do not suffer from the residual activity seen in DEIM simulations. The simulation time of DAPOD-DEIM with the present parameters is greater than the original model.

Finally, the bottommost plot in Figure 2 displays MOR results from the ADEIM method [20]. We used a look-back window length of $w = 25$ and $s_p = 10$ additional random sampling points in our simulations. The results resemble those of the DAPOD method, as the residual activity toward the end of simulation is correctly absent. The last activity peak occurs too early, and some of the earlier peaks have a smaller magnitude than the original simulation. The first population activity bursts are recreated accuracy similar to LDEIM. With regards to simulation time, ADEIM is the heaviest to compute, having a runtime of over tenfold the original model.

V. DISCUSSION

There are several differences between prior MOR studies in neuroscience and our present work. We make the fol-

lowing comparison to publications [1], [7], [12], since those considered a biophysically detailed and morphologically complex neuron model. First, the present network model is built by coupling heterogeneous ODE systems, in comparison to reducing discretized PDEs as in the other studies. Second, in terms of system dynamics the above studies used a model of a single neural cell where an action potential was propagating as a result of current injection, whereas we now include multiple neurons that receive and process stimulus from several sources asynchronously. Third, biophysically our cells include more complexity due to a larger number of distinct ionic currents, heterogenic parameters and functionally specialized compartments over copying identical compartments to create the single cell model. To make a final distinction on network topology, we view the single cell models of [1], [7], [12] as networks of compartments; then, their connectivity is restricted to neighbouring compartments. On the other hand, our network of compartmental neurons allows random connectivity between any number of cells.

A neuron model with a reset condition was reduced in [2] using POD. There, the reset condition was used to create spiking behavior in a simple phenomenological model, whereas in our study a state-dependent jump condition was employed to implement a biophysical threshold to the synaptic NMDA current. In [2] it was concluded that significant offline efforts were needed to derive a reliable reduced model. Our implementation of the state-dependent jump is explained in detail in Section III. We found that the jump condition reduces the computational efficiency of our reduced models. It can also be a major source of reduction error, if the jumps in reduced models occur at different timesteps than in the original model.

With the present model, reduction error grows rapidly as POD and DEIM dimensions get lower, which then prevents the reduction methods from achieving low dimensions with meaningful results. However, the reduction methods described in this study were able to replicate the emergent synchronized population activity seen in our original network model. This is an encouraging result, especially as these methods have originally been reported in the context of discretized PDE systems [4]. In comparison, our model is based on nonlinearly coupled heterogeneous neurons described by nonlinear ODEs, making the model reduction setting different from those in the MOR method publications.

Based on our study, DAPOD and ADEIM perform best in preserving the spiking activity of the original network model. However, ADEIM is too slow to be practically usable, as the present model does not allow low enough dimensions to offset the computational costs of online adaptivity. DAPOD is able to find a lower dimensional POD basis online than the other methods find offline, and has runtime close to the original model. We deem DAPOD especially useful if the system has "quiet" and "active phases", where the slowly evolving system could be approximated with a relatively small POD basis and when system-wide activity starts, POD dimension can increase to maintain a low error.

A shift in oscillation frequency, magnitude or phase of

population activity is a phenomenon seen in the reduced order models we presented in Section IV, Figure 2. It is difficult to exactly quantify the significance of this reduction error. However, with the relatively small computational efficiency increases seen in this study, the error is difficult to justify. The additional or missing population bursts in some of the reduced models are of greater significance. From the perspective of neuroscience, such behavior could be caused by intracellular or extracellular factors. The reduced models would not allow the study of these conditions, if they recreate an incorrect number of bursts of spikes.

We found residual network activity in DEIM and LDEIM models, seen as continued spiking activity towards the end of the simulation when the original model is no longer spiking. This reduction artifact could be caused by noise amplification as described in [19]. Especially the delicate ion channel kinetics are sensitive to approximation errors and noise. Interestingly, the two methods that adapt the reduced basis online, DAPOD-DEIM and ADEIM, do not display the same residual activity seen in DEIM and LDEIM reduced models with the same dimension. This improvement in accuracy does come at a cost in simulation speed.

VI. CONCLUSIONS AND FUTURE STUDIES

We constructed a network model of biophysically detailed compartmental neurons modeled with nonlinear ordinary differential equations, implemented several projection-based model order reduction methods and qualitatively evaluated model reduction results. When the model is stimulated with a current pulse, it displays synchronized population activity. The model was reduced with DEIM, LDEIM, DAPOD-DEIM and ADEIM. The reduced models had challenges in recreating the desired population behavior with low dimensions, possibly due to delicate ion channel kinetics or the inclusion of state-dependent jump conditions. Simulation was most efficient with DEIM, although DAPOD-DEIM and ADEIM capture the behavior of the model more accurately.

Future work will compare these results to reduced models obtained with TLDEIM [3] and the methods presented in [19].

REFERENCES

[1] D. Amsallem and J. Nordström. Energy stable model reduction of neurons by nonnegative discrete empirical interpolation. *SIAM Journal on Scientific Computing*, 38(2):B297–B326, 2016.

[2] M. Boulakia, E. Schenone, and J-F. Gerbeau. Reduced-order modeling for cardiac electrophysiology. Application to parameter identification. *International Journal for Numerical Methods in Biomedical Engineering*, 28(6-7):727–744, 2012.

[3] S. Chaturantabut. Temporal localized nonlinear model reduction with a priori error estimate. *Applied Numerical Mathematics*, 119:225–238, 2017.

[4] S. Chaturantabut and D. Sorensen. Nonlinear model reduction via discrete empirical interpolation. *SIAM Journal on Scientific Computing*, 32(5):2737–2764, 2010.

[5] E. Chmiel, J. Birgiolas, P. Gleeson, and W. Lytton. Pinsky and Rinzel 1994 CA3 neuron model. http://www.opensourcebrain.org/projects/ pinskyrinzelmodel,https://senselab.med.yale.edu/ ModelDB/ShowModel.cshtml?model=35358. Accessed 2019-02-19.

[6] Z. Drmac and S. Gugercin. A new selection operator for the discrete empirical interpolation method—improved a priori error bound and extensions. *SIAM Journal on Scientific Computing*, 38(2):A631–A648, 2016.

[7] B. Du, D. Sorensen, and S.J. Cox. Model reduction of strong-weak neurons. *Frontiers in Computational Neuroscience*, 8(164), 2014.

[8] N. Emamy, P. Litty, T. Klotz, M. Mehl, and O. Röhrle. POD-DEIM model order reduction for the monodomain reaction-diffusion submodel of the neuro-muscular system. In J. Fehr and B. Haasdonk, editors, *IUTAM Symposium on Model Order Reduction of Coupled Systems, Stuttgart, Germany, May 22–25, 2018*, pages 177–190, Cham, 2020. Springer International Publishing.

[9] W. Gerstner, H. Sprekeler, and G. Deco. Theory and simulation in neuroscience. *Science*, 338, 2012.

[10] A. Hodgkin and A. Huxley. A quantitave description of membrane current and its application to conduction and excitation in nerve. *Journal of Physiology*, 117(4):500–544, 1952.

[11] E. M. Izhikevich. Simple model of spiking neurons. *IEEE Transactions on Neural Networks*, 14(6):1569–1572, 2003.

[12] A. Kellems, S. Chaturantabut, D. Sorensen, and S. Cox. Morphologically accurate reduced order modeling of spiking neurons. *Journal of Computational Neuroscience*, 28(3), 2010.

[13] M. Lehtimäki, L. Paunonen, S. Pohjolainen, and M-L. Linne. Order reduction for a signaling pathway model of neuronal synaptic plasticity. *IFAC-PapersOnLine*, 50(1):7687–7692, 2017.

[14] J. Lumley, G. Berkooz, and P. Holmes. The Proper Orthogonal Decomposition in the analysis of turbulent flows. *Annual Review of Fluid Mechanics*, 25:539–575, 1993.

[15] A. Marasco, A. Limongiello, and M. Migliore. Fast and accurate low-dimensional reduction of biophysically detailed neuron models. *Scientific Reports*, 2:928, 2012.

[16] A. Marasco, A. Limongiello, and M. Migliore. Using Strahler's analysis to reduce up to 200-fold the run time of realistic neuron models. *Scientific Reports*, 3:2934, 2013.

[17] M Mordhorst, T. Strecker, D. Wirtz, T. Heidlauf, and O. Röhrle. Poddeim reduction of computational emg models. *Journal of Computational Science*, 19:86–96, 2017.

[18] B. Peherstorfer, D. Butnaru, K. Willcox, and H.J. Bungartz. Localized discrete empirical interpolation method. *SIAM Journal on Scientific Computing*, 36(1), 2014.

[19] B. Peherstorfer, Z. Drmač, and S. Gugercin. Stabilizing discrete empirical interpolation via randomized and deterministic oversampling. *arXiv preprint arXiv:1808.10473*, 2018.

[20] B. Peherstorfer and K. Willcox. Online adaptive model reduction for nonlinear systems via low-rank updates. *SIAM Journal on Scientific Computing*, 37(4), 2015.

[21] P. F. Pinsky and J. Rinzel. Intrinsic and network rhythmogenesis in a reduced traub model for CA3 neurons. *Journal of Computational Neuroscience*, 1(1-2):39–60, 1994.

[22] W. Rall. Theory of physiological properties of dendrites. *Annals of the New York Academy of Sciences*, 96(4):1071–1092, 1962.

[23] L. Sirovich. Turbulence and the dynamics of coherent structures. I-III. *Quarterly of Applied Mathematics*, 45(3):561–590, 1987.

[24] P. Tiso and D. J. Rixen. Discrete empirical interpolation method for finite element structural dynamics. In *Topics in Nonlinear Dynamics, Volume 1*, pages 203–212. Springer, 2013.

[25] R. D Traub, R. K. Wong, R. Miles, and H. Michelson. A model of a CA3 hippocampal pyramidal neuron incorporating voltage-clamp data on intrinsic conductances. *Journal of Neurophysiology*, 66(2):635–650, 1991.

[26] D. Wirtz, D. C. Sorensen, and B. Haasdonk. A posteriori error estimation for deim reduced nonlinear dynamical systems. *SIAM Journal on Scientific Computing*, 36(2):A311–A338, 2014.

[27] H. Yang and A. Veneziani. Efficient estimation of cardiac conductivities via pod-deim model order reduction. *Applied Numerical Mathematics*, 115:180–199, 2017.

[28] M. Yang and A. Armaou. Dissipative distributed parameter systems on-line reduction and control using DEIM/APOD combination. In *2018 Annual American Control Conference (ACC)*, pages 2557–2562. IEEE, 2018.

[29] M. Yang and A. Armaou. Revisiting APOD accuracy for nonlinear control of transport reaction processes: A spatially discrete approach. *Chemical Engineering Science*, 181:146–158, 2018.